Field-induced XY and Ising ground states in a quasi-two-dimensional $S = \frac{1}{2}$ Heisenberg antiferromagnet

Yoshimitsu Kohama,[1,*] Marcelo Jaime,[1] Oscar E. Ayala-Valenzuela,[1] Ross D. McDonald,[1] Eun Deok Mun,[1] Jordan F. Corbey,[2] and Jamie L. Manson[2]

[1]*MPA-CMMS, Los Alamos National Laboratory, Los Alamos, New Mexico 87545, USA*

[2]*Department of Chemistry and Biochemistry, Eastern Washington University, Cheney, Washington 99004, USA*

(Received 3 October 2011; revised manuscript received 11 October 2011; published 4 November 2011)

High field specific heat up to 35 T, C_p, and magnetic susceptibility, χ, measurements were performed on the quasi-two-dimensional (2D) Heisenberg antiferromagnet $[Cu(pyz)_2(pyO)_2](PF_6)_2$. While no C_p anomaly is observed down to 0.5 K in zero magnetic field, the application of field parallel to the crystallographic *ab*-plane induces a lambda-like anomaly in C_p, suggesting Ising-type magnetic order. On the other hand when the field is parallel to the *c*-axis, C_p and χ show evidence of *XY*-type antiferromagnetism. This dependence upon the field orientation occurs because the extreme two-dimensionality allows the intrinsic (zero field) spin anisotropy to dominate the interlayer coupling, which has hitherto masked such effects in other materials.

DOI: 10.1103/PhysRevB.84.184402 PACS number(s): 75.40.Cx, 75.10.Jm, 75.50.Xx

I. INTRODUCTION

Two-dimensional Heisenberg antiferromagnets (2D-HAFM) have been intensely studied on both theoretical and experimental fronts for many years and are still topical due to newly discovered materials. In an early study Mermin and Wagner[1] demonstrated that strong fluctuations in a strictly 2D model prevent long-range ordering at finite temperature. However, the reduction of the spin dimensionality n [i.e., the change from Heisenberg ($n = 3$) to XY ($n = 2$) and Ising models ($n = 1$)] suppresses spin fluctuations and leads to different types of transitions and regimes at finite temperatures. If easy-plane (EP) anisotropy is introduced, the 2D-HAFM can be described as a 2D-XY antiferromagnet (2D-XYAFM) and a Kosterlitz-Thouless (KT) transition takes place as characterized by a broad peak in the specific heat vs temperature $C_p(T)$.[2,3] When easy-axis (EA) anisotropy is introduced, the system becomes a 2D-Ising antiferromagnet (2D-IAFM) and shows a second order phase transition as characterized by a lambda-type anomaly in $C_p(T)$.[4,5] Since an applied magnetic field, H, can mimic an effective EP anisotropy, as earlier demonstrated,[6,7] the combined effect of external H and intrinsic EA/EP anisotropy can be used to tune the ground state of HAFM systems. However, in most real magnetic systems the inter-plane exchange coupling (J') is generally sufficient to induce 3D ordering, thus preventing experimental observation of the crossover from 2D-HAFM to 2D-XYAFM and 2D-IAFM.[8] Hence it is highly desirable to find a system close enough to the 2D limit for the properties and phase transitions to be externally tuned.

In this manuscript we provide an example of both field-induced XY and Ising states in a highly anisotropic quasi-2D-HAFM, $[Cu(pyz)_2(pyO)_2](PF_6)_2$ (Fig. 1). High field C_p and χ measurements reveal that the spin anisotropy and resultant nature of the phase transition can be tuned by the orientation of an applied H relative to the EP. The spin anisotropy observed in this and related materials[9] originates from the residual spin-orbit coupling in the tetragonal crystal field. The observed g-factor anisotropy is $\sim$10%,[10] and because the exchange spin-anisotropy is a higher order perturbation, the EP anisotropy Δ is expected to be an order of magnitude smaller. However, the extremely small J' of the title compound enables observation of the effect of Δ on the phase transition.

The Hamiltonian describing a 2D-HAFM with finite EA or EP anisotropies in an external field is given by

$$\hat{\mathrm{H}} = J/2 \sum_{i,j} \left[\hat{S}_i^a \hat{S}_j^a + \hat{S}_i^b \hat{S}_j^b + (1-\Delta)\hat{S}_i^c \hat{S}_j^c\right] - g_z \mu_B H \sum_i \hat{S}_i^z, \tag{1}$$

where J represents the in-plane antiferromagnetic coupling, and the sum (i, j) is over all nearest neighbors. The isotropic 2D-HAFM corresponds with $\Delta = 0$, and the 2D-HAFM with EA and EP anisotropies are $\Delta < 0$ and $\Delta > 0$, respectively. H is applied along the z-direction, and the last term in (1) represents the Zeeman energy. If an external magnetic field is applied, the spins align perpendicular to it to minimize the free energy and simultaneously satisfy the AFM exchange interaction, resulting in a suppression of spin fluctuations. Thus, when H is applied along the c-axis ($z = c$), the spin fluctuations along z are suppressed, and the spin projection (order parameter) in the *ab* plane behaves as XY spin [see Fig. 2(a)]. Although the order parameter can be reduced as field increases, an external field breaks $O(3)$ symmetry in the 2D-HAFM and induces a 2D-XYAFM [as illustrated schematically in Fig. 2(a)]. Accordingly, Cuccoli *et al.* indicated that H mimics EP anisotropy in pure 2D-HAFM and induces a KT-like broad C_p peak as field increases [Fig. 2(b)].[3] They also predicted that this effective spin anisotropy, Δ in (1), scales quadratically with H as $\Delta \sim 0.1h^2$ for small fields ($h < 2$), where h is the normalized magnetic field $h \equiv g\mu_B H/(JS)$. In spite of the intense research in this area,[9–13] hitherto the quadratic field dependence has never been confirmed, likely due to the non-negligible value of interplane exchange interaction J' in real systems. By contrast, the application of H in the EP in the 2D-XYAFM ($\Delta > 0$, and $z = a, b$) restricts the rotation in the *ab*-plane and induces an Ising ground state [see Fig. 2(a)].[7] Since the in-plane spin fluctuations can be tuned by H, the degree of spin fluctuations in two directions (c and a or b) becomes similarly weak near the critical field H_{Ising}, at which point the Zeeman energy is equal to the intrinsic EP anisotropy.

 ©2011 American Physical Society

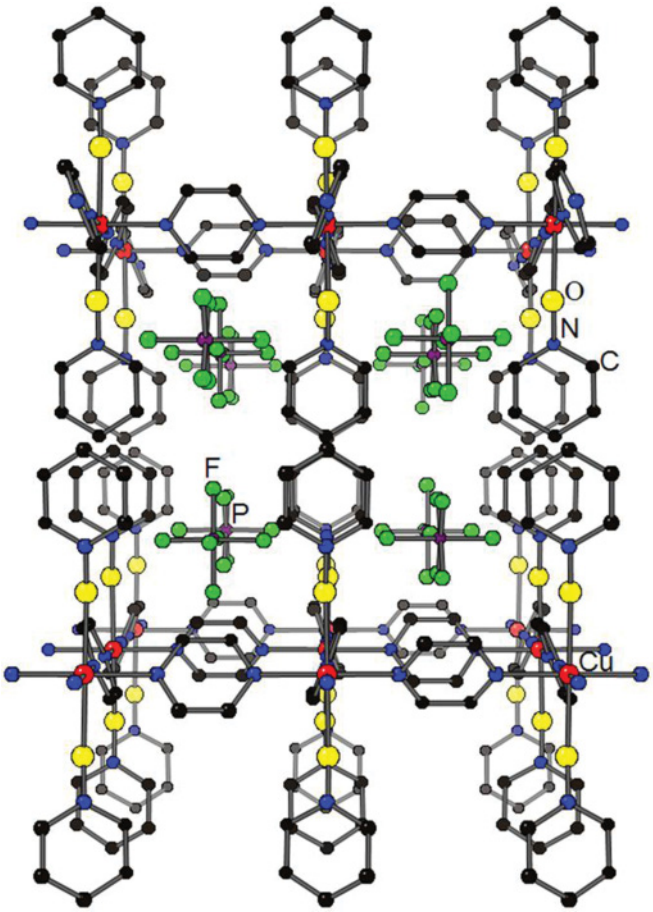

FIG. 1. (Color online) Room temperature structure of $[Cu(pyz)_2(pyO)_2](PF_6)_2$ as determined by single crystal x-ray diffraction. Hydrogen atoms have been omitted for clarity.

At $H = H_{\rm Ising}$, Eq. (1) can be reduced to

$$\hat{\rm H} = J/2 \sum_{i,j} \left[\hat{S}_i^b \hat{S}_j^b + (1-\Delta)\left(\hat{S}_i^a \hat{S}_j^a + \hat{S}_i^c \hat{S}_j^c\right)\right]. \qquad (2)$$

Equation (2) mimics the EA 2D-HAFM model for $\Delta > 0$ (compare with (1)),[7] suggesting the emergence of an Ising state in the *H*//*ab* case. It is interesting to note that the application of *H* parallel to the EA in 2D-IAFM can induce a spin-flop transition, which is not anticipated in the 2D-HAFM or *XY*AFM limits.[6]

$[Cu(pyz)_2(pyO)_2](PF_6)_2$ (pyz = pyrazine; pyO = pyridine-*N*-oxide) is a quasi-2D square-lattice AFM comprised of $[Cu(pyz)_2]^{2+}$ sheets (see Fig. 1). The material crystallizes in the orthorhombic space group *Cmca* with unit cell dimensions, $a = 13.7254(17)$, $b = 13.8278(17)$, $c = 26.377(3)$ Å, $V = 5006.1(11)$ Å^3 and $Z = 8$. The Cu(II) center is axially elongated along the O-Cu-O direction [Cu-O = 2.317(2) Å] with four nearly equivalent (and shorter) Cu-N bonds of 2.045(2) and 2.065(2) Å. The average intralayer Cu···Cu and shortest interlayer Cu···Cu separations are 6.889 and 13.683 Å, respectively. The structural qualities lead to $J' \ll J$ ($J' \sim 0.0017$ K, $J \sim 8.2$ K, and $J'/J \sim 2 \times 10^{-4}$), as determined by the experimental observables[10] $H_c^{\rm ab}$, $g^{\rm ab}$, and $T_{\rm N}$, which are given by $g\mu_{\rm B}H_c = 4J + 2J'$and $T_{\rm N} = 0.732\pi J/(2.43 - \ln(J'/J))$.[8] The high degree of structural (and exchange) anisotropy suggests $[Cu(pyz)_2(pyO)_2](PF_6)_2$ to be an excellent model of the 2D-HAFM.

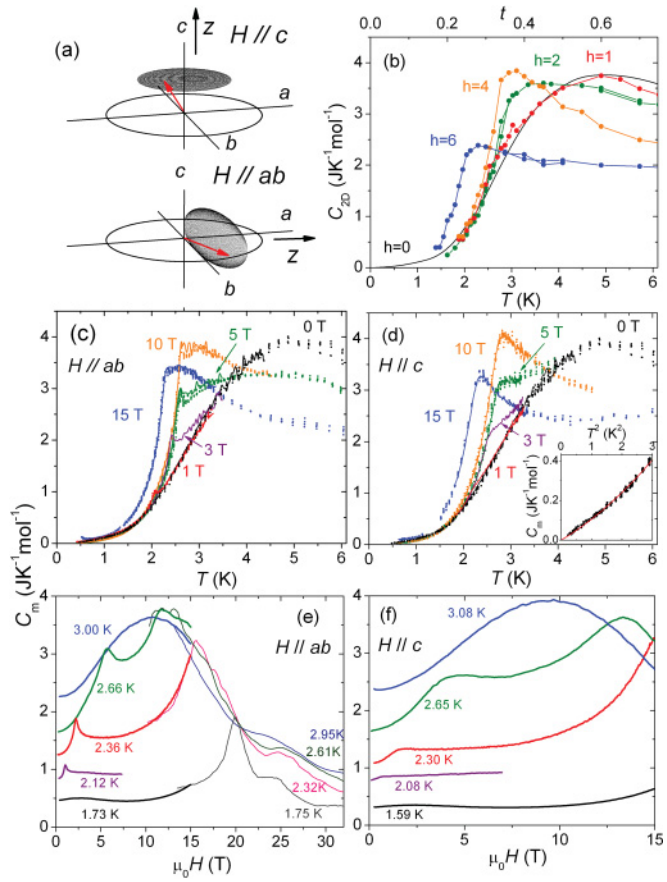

FIG. 2. (Color online) (a) Schematic illustrating the spin configuration of the field-induced *XY* (top), and Ising (bottom) states in weakly EP HAFM. The red-shadowed surface represents the direction at which spin can point out. In the case of isotropic HAFM, it is spherical. With positive Δ, the surface has a pancake-shape. When a strong *H* is applied perpendicular to the EP, the surface becomes disk-shaped, and the projection of spin on the *ab*-plane behaves as *XY* spin (top). If a weak *H* is in the EP, it restricts the spin fluctuation to the applied field orientation. Thus, the pancake-shape-allowed space becomes cigar-shaped, and the system can be approximated by the 2D-IAFM (bottom). (b) Predicted magnetic specific heat $C_{2D}(T)$ for a pure 2D-HAFM when *H*//*c*.[3,16] The theoretical temperature *t* was converted to *T* using $J/k_{\rm B} = 8.2$ K. (c), (d) Experimental $C_m(T)$ for *H*//*ab* and *H*//*c*. Here, solid lines were collected using the dual slope method, while dots were measured by the relaxation method. The inset of (d) shows C_m vs T^2 below 1.7 K. (e), (f) $C_m(H)$ for *H*//*ab* and *H*//*c*, measured with an AC technique, which was normalized to the data in (c), (d).

II. EXPERIMENTAL DETAILS

$C_p(H, T)$ and $\chi(H, T)$ were measured on single crystals of $[Cu(pyz)_2(pyO)_2](PF_6)_2$.[10] C_p vs *T* were obtained using both thermal relaxation and dual-slope techniques.[14] C_p vs *H* were measured using an AC technique.[15] $C_p(T,H)$ experiments were carried out in 15 T superconducting and 50 T pulsed magnets. The $\chi(H, T)$ experiments were performed with a Quantum Design PPMS. The magnetic contribution to the specific heat

$C_m(T)$ was obtained by subtracting the lattice specific heat estimated from high temperature data, as discussed in Ref. 12.

III. RESULTS AND DISCUSSIONS

Figures 2(c) and 2(d) show $C_m(T)$ for several H applied parallel and perpendicular to the 2D magnetic planes. In the absence of H we observe a smooth, featureless magnetic contribution, as expected for highly 2D systems. Indeed, the Monte Carlo simulations [black curve in Fig. 2(b)][3,16] indicate no features in the pure 2D-HAFM. Accordingly, we find that C_m follows the predicted power-law behavior for a pure 2D-HAFM, $C_m \sim aT^2 + bT^4$ in the low temperature limit [inset of Fig. 2(d)].[17]

The application of H induces features in C_m, which change shape according to the field intensity and orientation. For $H//c$ (i.e., normal to the 2D magnetic planes) broad peaks were observed. These broad peaks become much more prominent with increasing H, while the peak temperature first increases and then drops above ~7 T. The shape and increasing intensity of the peak in the high field region are similar to previous Monte Carlo results in pure 2D-HAFMs [Fig. 2(b)].[3] To make a quantitative comparison, we need to take into account an EP anisotropy $\Delta \approx 0.007$. From the expression $\Delta \sim 0.1h_p^2$[3] we introduce the effective field $h_{\rm eff} = h + h_p$, where Δ plays the role of an internal field $h_p \sim 0.26$. Then the applied magnetic field (0, 1, 3, 5, 10, and 15 T) can be written as $h_{\rm eff}$ (0.26, 0.64, 1.4, 2.1, 4.0, and 5.8). Our data show good agreement with numerical results at each corresponding $h_{\rm eff}$, providing strong evidence for field-induced XYAFM. It is important to note that the less anisotropic 2D-HAFMs[9,11] show sharp C_m peaks, which is evidence of 3D-ordering temperature (Néel transition), on top of the KT-like broad peak in all relevant magnetic fields. The absence of any sharp feature in the title compound is a direct consequence of the extremely high anisotropy.

When a small H (<5 T) is applied in the ab-plane, a characteristic λ-like peak is observed [Fig. 2(c)]. This λ-like anomaly can be seen on the low-temperature side of the broad peak. The λ-like peak for $H//ab$ is clearly observed in high resolution/high sensitivity $C_{\rm m}(H)$ measurements performed using an AC technique [Figs. 2(e) and 2(f) for $H//ab$ and $H//c$, respectively]. Indeed, at low fields the difference in $C_{\rm m}(H)$ between $H//ab$ and $H//c$ is remarkable. The $C_{\rm m}$ for $H//c$ only exhibits a shoulder-shaped anomaly. The field-induced λ-shaped anomaly observed for $H//ab$ is characteristic of Ising-type ordering and seems to evolve into a KT-type broad anomaly at higher fields. Although 3D-ordering can lead to a similar sharp peak, it is not expected in a very high anisotropy sample, e.g., $Sr_2CuO_2Cl_2$.[18] Additionally, a 3D Néel transition does not show field-orientation dependence, whereas the absence of a sharp peak for $H//c$ is inconsistent with such a transition. In addition a field-induced Ising state can be expected from Eq. (2) when an external field is applied to ab-plane. Thus, we interpret that the sharp peak is the signature of Ising-like transition. We note that the Monte Carlo method cannot be carried out for $H//ab$ due to the well-known sign problem. Consequently, further theoretical development is necessary in this area. At $H \sim 25$ T we also see a broad anomaly in $C_{\rm m}(H//ab)$. This broad anomaly arises from thermal excitations between magnetic spin levels, i.e., a Schottky anomaly, corresponding to the magnetization $M(H)$ saturation at ~24 T.[10]

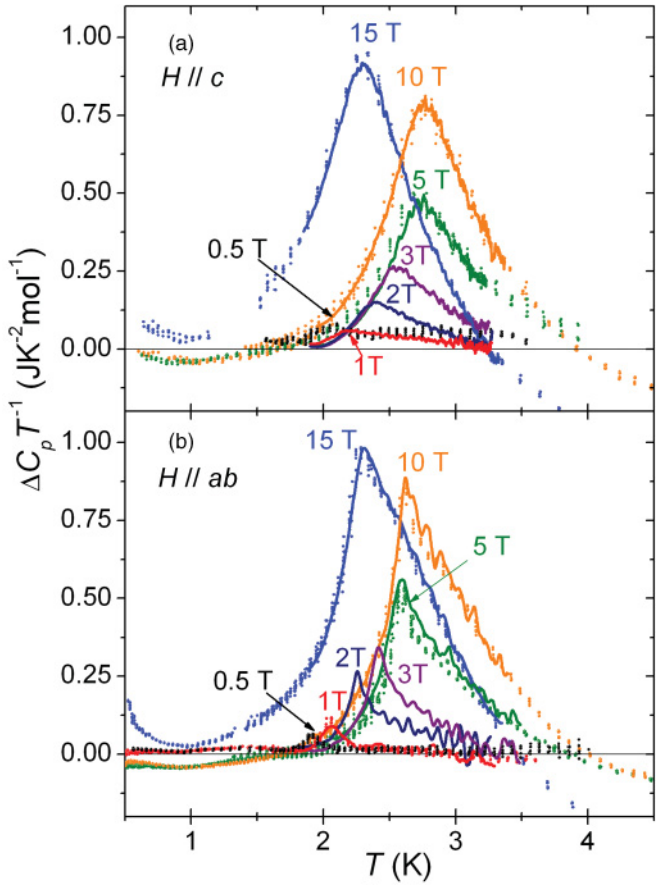

FIG. 3. (Color online) $\Delta C_p T^{-1}(T)$ for (a) $H//c$ and (b) $H//ab$. The upturn of $\Delta C_p(15\ {\rm T})T^{-1}$ below 1 K likely comes from a magnetic nuclear Schottky anomaly.

The magnetic contribution to C_p is determined by calculating the difference $\Delta C_p(T,H) = C_p(T,H) - C_p(T,0)$, and we plot $\Delta C_p T^{-1}$ in Fig. 3. Previous Monte Carlo simulations have shown that the magnitude of $\Delta C_p T^{-1}$ monotonically increases with H.[3,16] A clear confirmation of the prediction is seen in Fig. 3(a). Figure 3(b) reveals a sharper λ-like peak when a weak field $H//ab$ ($H \leqslant 3$T) is applied. Below 2 T, the peak height is roughly twice as high as the KT broad peak observed for $H//c$. However, above 5 T, the peak height is almost identical to the $H//c$ data. Since the order parameter (the XY component of spin) is reduced as field increases, this indicates that the intensity of the λ-anomaly is correlated with the magnitude of the order parameter.

Figure 4 shows the DC susceptibility $\chi(T) = M/H$ for $H//c$ and $H//ab$. In the low-field region χ shows a broad bump around 7.7 K, which is characteristic of the 2D-HAFM.[17] For both field orientations, an upturn is observed below $T = 3$ K. According to Monte Carlo simulations,[3] the minimum temperature ($T_{\rm min}$) in $\chi(T)$ marks the onset of XY behavior below $2h_{\rm eff}$ (~4.7 T) in the $H//c$ case. A similar minimum is also observed for $H//ab$, and both $T_{\rm min}$ for $H//ab$ and $H//c$ occur at temperatures slightly higher than the anomaly in ΔC_p, as indicated by arrows in Fig. 4. This behavior is expected

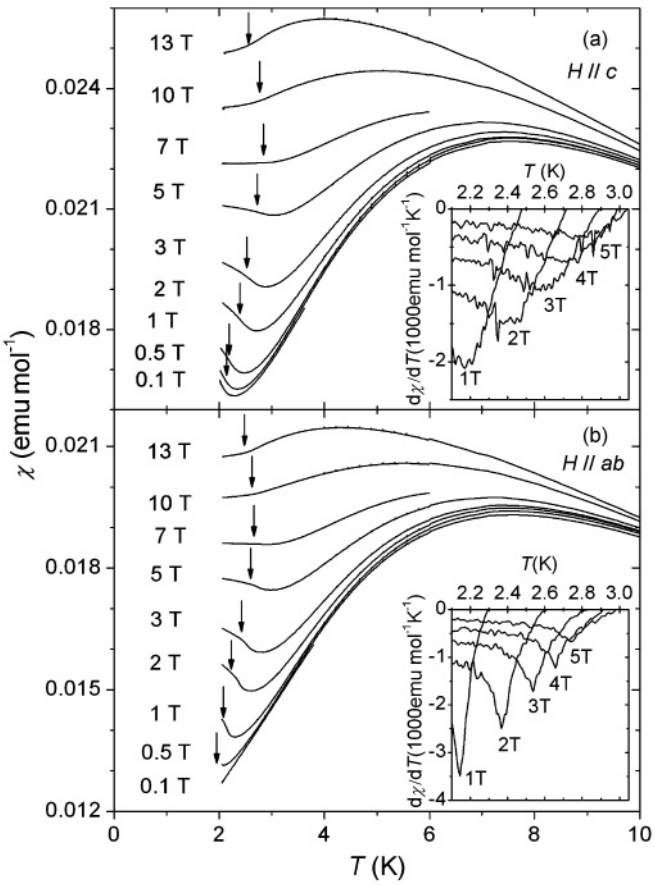

FIG. 4. $\chi(T)$ for (a) $H//c$ and (b) $H//ab$. The arrows indicate the peak temperature in ΔC. The insets show $\partial\chi(T)/\partial T$ below 5 T.

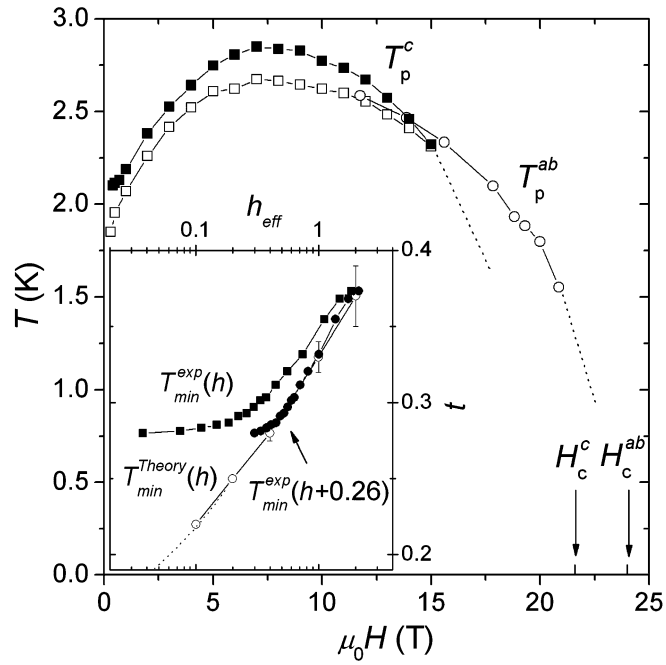

FIG. 5. T-H phase diagram for $H//c$ and $H//ab$. The solid and open symbols are the T_p for $H//c$ and $H//ab$. The inset compares our experimental $T_{\min}$ to theory. The horizontal and vertical axis are h_{eff} and normalized temperature ($t \equiv J/\text{K} = 8.2$ K). The open circles are the $T_{\min}$ from Monte Carlo simulation.[3] The solid circles and squares are the experimental $T_{\min}(h_{\text{eff}})$ with/without taking into account EP anisotropy.

for 2D-XYAFM and 2D-IAFM in the low field region.[3,5] The derivative $\partial\chi(T)/\partial T$ is plotted for both field orientations in the insets of Figs. 4(a) ans 4(b). While a sharp peak is seen for $H//ab$, just a broad feature is evident for $H//c$. We interpret the sharp peak as arising from the Ising nature of the magnetic transition. As H is increased, the peak becomes smaller and the difference between field orientations vanishes. Indeed, $\partial\chi(T)/\partial T$ at $H = 5$ T is similar for both $H//c$ and $H//ab$. As in the case of $C_m(T, H)$, a strong enough H reduces the amplitude of the order parameter, reducing the observable difference between $H//c$ and $H//ab$.

Most quasi-2D systems show anomalies in both C_p and χ.[9] By contrast, our data for $H//c$ reveal no $\chi(T)$ anomaly in the high field region in marked contrast to the large KT peak observed in $C_m(T)$, which grows with H. This behavior was identified in earlier Monte Carlo simulations as a signature of the magnetic field-induced 2D-XYAFM,[3] which can be understood from a microscopic point of view. The peak in $C_m(T)$ relates to the magnetic entropy, i.e., it is a measurement of the magnetic degrees of freedom in all directions. $\chi(T)$ measures the fraction of spins that are tilted in the applied field direction. The z-component of spin cannot fluctuate in high fields, and the vortex/antivortex creation at the KT transition is the ordering perpendicular to z axis, which cannot induce any anomaly in χ (z-spin component) but can change the degrees of freedom in the XY plane. This explains why our data show an obvious $C_m(T)$ anomaly and no $\chi(T)$ anomaly in the high field region and highlights our complementary measurements of C_p and χ.

Figure 5 displays the T-H phase diagram as obtained from our $C_p(T, H)$ measurements. A clear nonmonotonic dependence of T_p with respect to H was found as in other quasi-2D systems.[9,11] Sengupta *et al.*[11] proposed that the nonmonotonic behavior is caused by the phase fluctuations typical for a 2D system. Although it is probably possible to extract J and J' by fitting the T-H phase diagram to the theoretical result,[11] the difficulty to extract the KT transition temperature from C_p peaks prevents a quantitative comparison. Thus, we compare the experimental $T_{\min}^{\text{exp}}$ collected for $H//c$ to the theoretical $T_{\min}^{\text{theory}}$ in the inset of Fig. 5.[3] Here, the experimental $T_{\min}^{\text{exp}}$ is plotted as a function of h_{eff}. If we assume no EP anisotropy ($\Delta, h_{\text{p}} = 0$), $T_{\min}^{\text{exp}}$ shows a clear departure from the theory. However, if we take $h_{\text{p}} = 0.26$ ($\Delta = 0.007$), the agreement between $T_{\min}^{\text{exp}}$ and $T_{\min}^{\text{theory}}$ becomes significantly better. This value of the spin anisotropy is in good agreement with independent microwave frequency measurement of AFM resonance in this and related compounds.[9,10] The observed agreement confirms that the EP anisotropy acts as an external magnetic field and *vice versa*.

IV. CONCLUSIONS

In summary we have studied the field-induced XY and Ising ground states in the $S = 1/2$ weakly EP quasi-2D HAFM $[\text{Cu(pyz)}_2(\text{pyO})_2](\text{PF}_6)_2$ with $C_p(T, H)$ and $\chi(T, H)$ measurements. Since the H mimics an additional EP anisotropy, for

$H//c$, the system then displays an XY ground state. On the other hand when the H is applied parallel to the ab-plane, by the combination of the intrinsic EP anisotropy and the external H, an Ising ground state emerges. Finally, we emphasize that the field-induced behavior reported here very likely arises from the extreme two-dimensionality, i.e., an extremely weak $J'/J \sim 2 \times 10^{-4}$. In contrast the less anisotropic system $[Cu(pyz)_2(HF_2)]PF_6$ ($J'/J \sim 0.03$ and $\Delta \sim 0.003$[9]) shows a sharp anomaly in C_p and χ for all values and orientation of H, a signature of the traditional Néel transition. The first observation of field-induced 2D-XYAFM and 2D-IAFM physics is now demonstrated in $[Cu(pyz)_2(pyO)_2](PF_6)_2$.

ACKNOWLEDGMENTS

We acknowledge fruitful discussions with T. Roscilde, C. D. Batista, and J. Singleton. Y.K., M.J., E.M., O.A., and R.M. were supported by NSF, US-DOE, and the State of Florida. Work at EWU was supported by the National Science Foundation under Grant No. DMR-1005825.

*ykohama@lanl.gov

[1] N. D. Mermin and H. Wagner, Phys. Rev. Lett. **17**, 1133 (1966).
[2] J. M. Kosterlitz and D. J. Thouless, J. Phys. C **6**, 1181 (1973).
[3] A. Cuccoli, T. Roscilde, R. Vaia, and P. Verrucchi, Phys. Rev. B **68**, 060402(R) (2003).
[4] L. Onsager, Phys. Rev. **65**, 117 (1944).
[5] A. Cuccoli, T. Roscilde, V. Tognetti, R. Vaia, and P. Verrucchi, Phys. Rev. B **67**, 104414 (2003).
[6] D. P. Landau and K. Binder, Phys. Rev. B **24**, 1391 (1981).
[7] A. R. Pereira and A. S. T. Pires, Phys. Rev. B **51**, 996 (1995).
[8] C. Yasuda, S. Todo, K. Hukushima, F. Alet, M. Keller, M. Troyer, and H. Takayama, Phys. Rev. Lett. **94**, 217201 (2005).
[9] E. Čižmár, S. A. Zvyagin, R. Beyer, M. Uhlarz, M. Ozerov, Y. Skourski, J. L. Manson, J. A. Schlueter, and J. Wosnitza, Phys. Rev. B **81**, 064422 (2010).
[10] P. A. Goddard, J. L. Manson, J. Singleton, I. Franke, T. Lancaster, A. J. Steele, S. J. Blundell, C. Baines, F. L. Pratt, R. D. McDonald, O. A. Valenzuela, J. F. Corbey, H. I. Southerland, P. Sengupta, and J. A. Schlueter (in preparation).
[11] P. Sengupta, C. D. Batista, R. D. McDonald, S. Cox, J. Singleton, L. Huang, T. P. Papageorgiou, O. Ignatchik, T. Herrmannsdörfer, J. L. Manson, J. A. Schlueter, K. A. Funk, and J. Wosnitza, Phys. Rev. B **79**, 060409(R) (2009).
[12] J. L. Manson, J. A. Schlueter, K. A. Funk, H. I. Southerland, B. Twamley, T. Lancaster, S. J. Blundell, P. J. Baker, F. L. Pratt, J. Singleton, R. D. McDonald, P. A. Godard, P. Sengupta, C. D. Batista, L. Ding, C. Lee, M.-H. Whangbo, I. Franke, S. Cox, C. Baines, and D. Trial, J. Am. Chem. Soc. **131**, 6733 (2009).
[13] A. Orendáčová, E. Čižmár, L. Sedlakova, J. Hanko, M. Kajnakova, M. Orendac, A. Feher, J. S. Xia, L. Yin, D. M. Pajerowski, M. W. Meisel, V. Zelenak, S. Zvyagin, and J. Wosnitza, Phys. Rev. B **80**, 144418 (2009).
[14] A. A. Aczel, Y. Kohama, M. Jaime, K. Ninios, H. B. Chan, L. Balicas, H. A. Dabkowska, and G. M. Luke, Phys. Rev. B **79**, 100409(R) (2009).
[15] Y. Kohama, C. Marcenat, T. Klein, and M. Jaime, Rev. Sci. Instrum. **81**, 104902 (2010).
[16] T. Roscilde (private communication).
[17] J. K. Kim and M. Troyer, Phys. Rev. Lett. **80**, 2705 (1998).
[18] P. Sengupta, A. W. Sandvik, and R. R. P. Singh, Phys. Rev. B **68**, 094423 (2003).